

# Frequency-domain versus time-domain imaging for photonics-based broadband radar

Guanqun Sun, Fangzheng Zhang<sup>✉</sup>, Shilong Pan and Xingwei Ye

Photonics-based radar enables a large operation bandwidth that is particularly favourable for high-resolution synthetic aperture imaging. However, how to implement fast and high-accuracy imaging with photonics-based broadband radar is still an open question. In this Letter, the performance of photonics-based inverse synthetic aperture radar imaging with frequency-domain and time-domain algorithms are experimentally investigated and compared. The results show that, frequency-domain range-Doppler algorithm has fast imaging capability, but the image suffers from defocusing and distortions. Although migration compensation techniques can be applied to improve the imaging accuracy, the imaging speed is significantly reduced. On the other hand, using time-domain back-projection (BP) algorithm can achieve well-focused images, and the imaging speed can be enhanced with fast BP methods. Therefore, the time-domain imaging method is found to be the best choice for fast and high-accuracy synthetic aperture imaging with photonics-based broadband radars.

**Introduction:** In recent years, photonics-based radar has attracted lots of attention, because its large operation bandwidth is highly desirable for high-resolution imaging [1, 2]. Previously, photonics-based inverse synthetic aperture radar (ISAR) imaging has been successfully demonstrated [3–6], in which the resolution reaches as high as  $2\text{ cm} \times 2\text{ cm}$ . In these demonstrations, frequency-domain range-Doppler (RD) algorithm is applied to construct the image with a fast speed. Although the RD algorithm is widely used in narrow-band radar imaging, it may not be the best choice for photonics-based broadband radar imaging in which the migration effect is serious because of the high range resolution. Migration compensation techniques, such as the keystone transform [7], provide possible solutions to this problem, but the compensation accuracy is limited and the increased computation complexity will reduce the imaging speed. On the other hand, radar imaging with time-domain back-projection (BP) algorithm can solve the migration problem with accurate coherent accumulation. However, BP algorithm has a high computation complexity that leads to a slow imaging speed. Fortunately, a few fast BP (FBP) algorithms have been proposed to enhance the imaging speed [8]. Therefore, time-domain BP algorithm is still attractive, especially for broadband radar imaging. In this Letter, we experimentally investigate the performance of photonics-based ISAR imaging using frequency-domain RD algorithm and time-domain BP algorithm, respectively. The result can provide a guideline for photonics-based broadband radar to achieve high accuracy and fast imaging.

**Experimental setup:** The photonics-based radar is established based on photonic frequency multiplication and photonic frequency mixing [9], of which the schematic diagram is shown in Fig. 1a. The continuous-wave light from a laser diode (TeraXion Inc., 1550.12 nm) is modulated by a dual-parallel Mach-Zehnder modulator (DPMZM, Fujitsu FTM7962EP). A voltage-controlled oscillator (INNO-9205) is used to generate a linearly frequency-modulated (LFM) signal, of which the bandwidth is 2 GHz (4.5–6.5 GHz) and the pulse width is 100  $\mu\text{s}$  with a repetition rate of 5 kHz. This LFM signal passes through an electrical 90° hybrid coupler, and the two output signals are sent to the two RF ports of the DPMZM. After properly setting the bias voltage, the DPMZM works in frequency quadrupling mode [9]. The obtained optical signal is divided into two branches by an optical coupler. In the upper branch, the optical signal is sent to photodetector (PD1, u2t XPDV2120RA, bandwidth: 40 GHz) to generate a frequency quadrupled LFM signal from 18 to 26 GHz [9]. This LFM signal is amplified by an electrical amplifier (EA1, SHF 806E, 26 dB gain) before emitted by the transmit antenna (Tx). In the lower branch, the signal is used as a reference in the receiver, where the radar echoes are collected by the receive antenna (Rx) and amplified by another amplifier (EA2). The optical reference is modulated by the radar echoes at an MZM (EOSAPCE Inc.). The output signal is amplified by an erbium-doped optical fibre amplifier and sent to another PD (PD2, CONQUER Inc., bandwidth: 10 GHz) to implement photonic frequency de-chirping [9].

An electrical low-pass filter is followed to remove the high-frequency interference, and the desired de-chirped signal is sampled by an analogue-to-digital converter before processed in a digital signal processing unit. The packaged radar is shown in Fig. 1b. Its operation bandwidth is 8 GHz (18–26 GHz), and the theoretical range resolution is 1.875 cm.

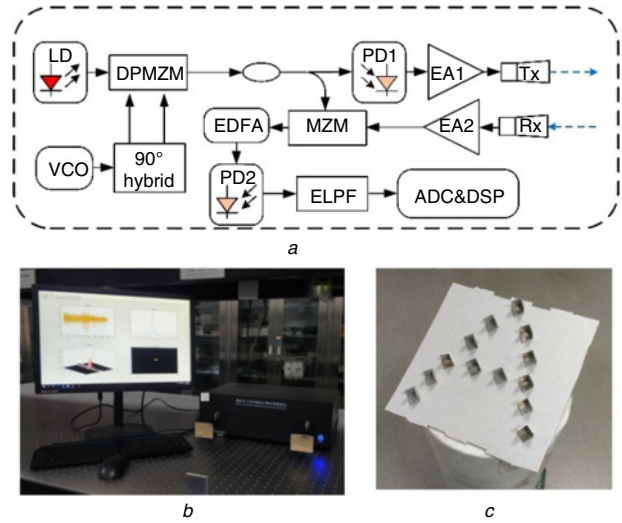


**Fig. 1** Photonics-based radar and target  
a Schematic diagram of the photonics-based radar  
b Photograph of the packaged radar  
c Target used in the ISAR imaging experiment

The imaging target is composed of 13 small reflectors (size of each reflector:  $2\text{ cm} \times 2\text{ cm} \times 2\text{ cm}$ ) composing the shape of a letter ‘A’, as shown in Fig. 1c. The target is placed on a turntable with a rotation speed of  $\omega = 360^\circ/\text{s}$ , of which the geometry is shown in Fig. 2. The distance between the radar and the rotation centre  $O$  is  $R_o = 1.5\text{ m}$ .  $P$  is a scatter point at  $(x_i, y_i)$ , and its rotational angle with respect to  $X$ -axis is  $\theta$  at azimuth time  $t_i$  ( $\theta = \omega t_i$ ). The instantaneous range from the scatter point  $P$  to the radar is given by

$$R_p(t_i) = R_o + x_i \sin \omega t_i + y_i \cos \omega t_i \quad (1)$$

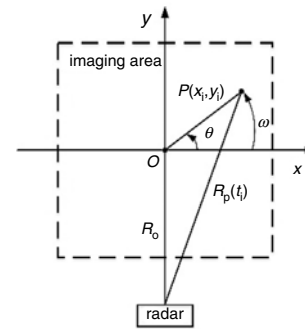


**Fig. 2** Turntable ISAR imaging geometry

The de-chirped radar echoes of the scatter can be expressed as

$$\begin{aligned} s(\tau, t_i) &= \text{rect}\left(\frac{\tau - (2R_p(t_i)/c)}{T}\right) \exp\left\{-j4\pi k \frac{R_p(t_i)}{c} \tau\right\} \exp\left\{-j4\pi f_c \frac{R_p(t_i)}{c}\right\} \\ &= \text{rect}\left(\tau - \frac{2(R_o + x_i \sin \omega t_i + y_i \cos \omega t_i)}{c}\right) / T \\ &\quad \times \exp\left\{-j \frac{4\pi}{c} (k\tau + f_c)(R_o + x_i \sin \omega t_i + y_i \cos \omega t_i)\right\} \end{aligned} \quad (2)$$

where  $c$  is the speed of light,  $T$  is the pulse width of the transmitting signal,  $k$  is the chirp rate,  $\tau$  is the fast time of the range and  $f_c$  is the radar carrier frequency. In the experiments using both frequency-domain

and time-domain ISAR imaging algorithms, the coherent processing interval is fixed to achieve an equivalent observation angle of  $40^\circ$ , which corresponds to a theoretical azimuth resolution of 0.99 cm.

*ISAR imaging with RD algorithm:* The range profile is obtained by performing fast Fourier transformation (FFT) to the de-chirped signal in (2). When doing this, the following approximation is made based on Taylor expansion:

$$\begin{aligned}\sin \omega t_i &\approx \omega t_i - \frac{1}{6} \omega^3 t_i^3 \\ \cos \omega t_i &\approx 1 - \frac{1}{2} \omega^2 t_i^2\end{aligned}\quad (3)$$

In narrow-band ISAR imaging with RD algorithm, the envelope shift due to the term of  $x_i(\omega t_i - \omega^3 t_i^3/6) - y_i(\omega^2 t_i^2/2)$  is ignored because it is much less than the range resolution unit. With this approximation, the range profile can be expressed as

$$s_{RD}(\tau, t_i) \propto \text{sinc}\left\{Tk\left(\tau - \frac{2(R_o + y_i)}{c}\right)\right\} \exp\left(-j\frac{4\pi f_c}{c}x_i\omega t_i\right)\quad (4)$$

The final image can be obtained by operating azimuth FFT to (4)

$$s_{RD}(\tau, f_i) \propto \text{sinc}\left\{Tk\left(\tau - \frac{2(R_o + y_i)}{c}\right)\right\} \text{sinc}\left\{T_a\left(f_i - \frac{2f_c}{c}x_i\omega\right)\right\}\quad (5)$$

where  $f_i$  is the Doppler frequency in azimuth direction and  $T_a$  is the observation interval.

Fig. 3a shows the image constructed by RD algorithm using a computer with an Intel i5-8500 CPU (6-core) and a DDR4 RAM (16 GB). The imaging time is recorded to be 0.062 s. In Fig. 3a, the shape of letter A can be easily observed, but obvious defocusing and distortions appear especially for the scatters away from the rotation centre. This is caused by the fact that the large operation bandwidth of the photonics-based radar leads to distance migration across a large number of range resolution units. In this case, more terms in (3) should be considered to acquire accurate range profiles. When the first-order keystone transform with an eight-point truncated sinc interpolation is used to compensate for the migration [7], the obtained image is shown in Fig. 3b, where the focusing accuracy is apparently improved for the scatters close to the rotation centre. While, the scatters far from the rotation centre still suffer from defocusing and distortions. Due to the high computation complexity of the keystone transform, the entire imaging time is increased to 0.228 s. If higher-order keystone transform is applied, the imaging accuracy is expected to be further improved, but this will bring substantial increase on the complexity and imaging time.

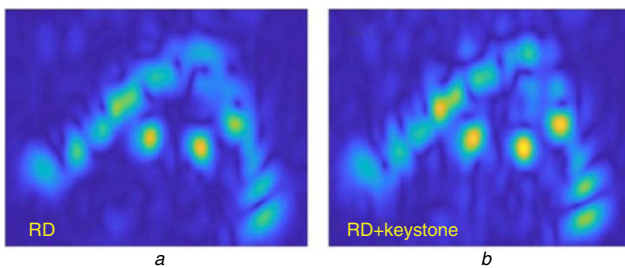


**Fig. 3** Image obtained by  
a RD algorithm  
b RD algorithm with the first-order keystone transform

*ISAR imaging with BP algorithm:* First, pulse compression by FFT operation is performed to obtain range profiles in different azimuth time. Based on these range profiles, the amplitudes at each pixel of the imaging area can be obtained through interpolation. The obtained coarse images of different azimuth time are coherently accumulated layer by layer to get the final image [8]. Since BP algorithm only considers the delay information, it avoids the approximation in (3) and does not have the problem of migration correction. Thus, it is more suitable for photonics-based radar imaging with large operation bandwidth.

Fig. 4a shows the image constructed by BP algorithm. Compared with the images in Fig. 3, the BP image has much better performance,

in which the energy is accurately focused on all the scatters. The imaging time for BP algorithm is measured to be 5.364 s, indicating the imaging speed is much slower than that of RD algorithm. To enhance the imaging speed, we use the FBP method as proposed in [8]. The imaging result is shown in Fig. 4b. As can be observed, the FBP image is slightly deteriorated compared with the BP image, but it still has better focusing performance than the images in Fig. 3. The imaging time of the FBP method is measured to be 0.174 s, which is even faster than the method by RD algorithm with keystone transform.

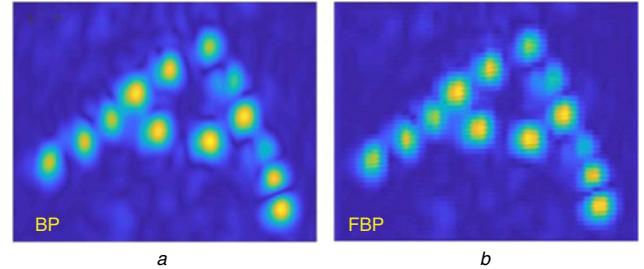


**Fig. 4** Image obtained by  
a BP algorithm  
b FBP algorithm

*Conclusion:* For photonics-based broadband ISAR imaging, although the frequency-domain RD algorithm can achieve a fast imaging speed, the scatters away from the rotation centre suffer from serious defocusing and distortions. When using migration compensation techniques to solve this problem, the advantage of fast imaging does not exist. The time-domain BP algorithm can achieve well-focused images. Using FBP methods, the imaging speed can be comparable with the RD algorithm with migration compensation. Therefore, the time-domain BP algorithm is the best choice to construct high-accuracy images with acceptable imaging speed for photonics-based broadband radars.

*Acknowledgments:* This work was supported in part by the National Natural Science Foundation of China under grant 61871214, in part by the Natural Science Foundation of Jiangsu Province under grant BK20180066, in part by the Jiangsu Provincial Program for High-level Talents in Six Areas under grant DZXX-005 and in part by the Foundation of Graduate Innovation Centre in NUAA (kfj20190401).

© The Institution of Engineering and Technology 2020  
Submitted: 04 August 2020 E-first: 29 October 2020  
doi: 10.1049/el.2020.2273

One or more of the Figures in this Letter are available in colour online.

Guanqun Sun, Fangzheng Zhang, Shilong Pan and Xingwei Ye (*College of Electric and Information Engineering, Nanjing University of Aeronautics and Astronautics, Nanjing 210016, People's Republic of China*)

✉ E-mail: zhangfangzheng@nuaa.edu.cn

## References

- Ghelfi, P., Laghezza, F., Scotti, F., *et al.*: 'Photonics in radar systems: rf integration for state-of-the-art functionality', *IEEE Microw. Mag.*, 2015, **16**, (8), pp. 74–83
- Ghelfi, P., Laghezza, F., Scotti, F., *et al.*: 'A fully photonics-based coherent radar system', *Nature*, 2014, **507**, p. 341
- Li, R., Li, W., Ding, M., *et al.*: 'Demonstration of a microwave photonic synthetic aperture radar based on photonic-assisted signal generation and stretch processing', *Opt. Express*, 2017, **25**, (13), pp. 14334–14340
- Peng, S., Li, S., Xue, X., *et al.*: 'High-resolution W-band isar imaging system utilizing a logic-operation-based photonic digital-to-analog converter', *Opt. Express*, 2018, **26**, (2), pp. 1978–1987
- Zou, W., Zhang, H., Long, X., *et al.*: 'All-optical central-frequency-programmable and bandwidth-tailorable radar', *Sci. Rep.*, 2016, **6**, p. 19786

- 6 Ye, X., Zhang, F., Yang, Y., *et al.*: 'Photonics-based radar with balanced I/Q de-chirping for interference-suppressed high-resolution detection and imaging', *Photon. Res.*, 2019, **7**, (3), pp. 265–272
- 7 Yang, L., Xing, M., Zhang, L., *et al.*: 'Integration of rotation estimation and high-order compensation for ultrahigh-resolution microwave photonic isar imagery', *IEEE Trans. Geosci. Remote Sens.*, 2020, to appear, pp. 1–21, doi: 10.1109/TGRS.2020.2994337
- 8 Sun, G., and Zhang, F.: 'Convolutional neural network (cnn)-based fast back projection imaging with noise-resistant capability', *IEEE Access*, 2020, **8**, pp. 117080–117085
- 9 Zhang, F., Guo, Q., and Pan, S.: 'Photonics-based real-time ultra-high-range-resolution radar with broadband signal generation and processing', *Sci. Rep.*, 2017, **7**, (1), p. 13848